

Entanglement entropy, phase transition, and island rule for Reissner-Nordström-AdS black holes

Shu-Yi Lin,¹ Ming-Hui Yu,¹ Xian-Hui Ge^{1,2,*} and Li-Jun Tian¹

¹*Department of Physics, Shanghai University, Shanghai 200444, People's Republic of China*

²*Institute for Quantum Science and Technology, Shanghai University, Shanghai 200444, People's Republic of China*



(Received 27 May 2024; accepted 8 July 2024; published 7 August 2024)

This study focuses on the examination of the island rule within the context of four-dimensional Reissner-Nordström-anti-de Sitter (4D RN-AdS) black holes, illuminating the intricate relationship between the entanglement entropy and phase transitions of black holes. The entanglement entropy of 4D RN-AdS black holes follows the anticipated linear growth pattern before ultimately declining to a constant value, in accordance with the well-established Page curve. The novelty of this study lies in the examination of the influence, previously unexplored, of the first-order phase transition on the shape and evolution of the Page curve in situations involving both eternal and evaporating black holes. Despite the morphological alterations of the curve induced by the transition, the inherent unitarity of the system persists. As the evaporation progresses, the Page curve displays diverse configurations, unveiling phenomena that are novel and defies traditional expectations, thereby enriching our comprehension of the thermodynamics of black holes interlinked with quantum information.

DOI: [10.1103/PhysRevD.110.046008](https://doi.org/10.1103/PhysRevD.110.046008)

I. INTRODUCTION

The black hole information paradox [1] is one of the most fundamental problems to be solved in theoretical physics. Its origin lies in our comprehensive understanding of quantum gravity, and the resolution of the information paradox is fundamentally dependent on a thorough comprehension of quantum gravity. To elucidate this concept, we consider a scenario in which the collapse of a star into a black hole leads to an initial radiation state represented by the quantum state $|\Psi\rangle$. By means of the gravitational path integral, this initial state $|i\rangle$ transitions into the final state $|j\rangle$, a process that encompasses Hawking radiation [1–3]. To compute the von Neumann entropy of the black hole radiation, one can utilize the replica trick, which involves considering n copies of the system, to compute the Renyi entropy, then taking the $n \rightarrow 1$ limit. The Renyi entropy is expressed as

$$S = -\lim_{n \rightarrow 1} \frac{1}{n-1} \log \text{Tr}(\rho^n), \quad (1.1)$$

*Contact author: gexh@shu.edu.cn

Published by the American Physical Society under the terms of the [Creative Commons Attribution 4.0 International](https://creativecommons.org/licenses/by/4.0/) license. Further distribution of this work must maintain attribution to the author(s) and the published article's title, journal citation, and DOI. Funded by SCOAP³.

where ρ as the density matrix of either the black hole or the radiation, and it is possible to compute the Renyi entropies in a way that has a good continuation in n . The density matrix can be represented as $\rho = |\Psi\rangle\langle\Psi|$, and the matrix elements ρ_{ij} as $\langle i|\Psi\rangle\langle\Psi|j\rangle$. For $n \neq 1$, the interior of the black hole can exhibit diverse connections among the n replicas [4]. At the early times, the Hawking saddle dominates the process, it would lead to the Hawking curve, and the density matrix ρ is a thermal state or a mixed state. While at the late times, the replica wormholes saddle dominates the process, leading to the unitary Page curve [5,6]. The state of the black hole corresponds to a pure state of density matrix ρ .

The complete entanglement entropy curve of a unitary evaporating black hole follows the Page curve [7], as recently solved by the island rule [8–11]. The Page curve describes the entropy of Hawking radiation, arising from the interplay between two saddle solutions: the Hawking saddle and the replica wormholes saddle [12]. The former is characterized by the von Neumann entropy, S_{bulk} , which shows a perpetual linear increase, reflecting the ongoing complexity within Hawking's computation [13]. The latter reflects the entropy defined by the island rule, associated with Renyi entropy or the Bekenstein-Hawking entropy. According to Page's theorem, the entropy of a bipartite quantum system in a random pure state is given by [7,14]

$$S(R) = \min(\log d_R, \log d_B), \quad (1.2)$$

where d_R and d_B denote the dimensions of the Hilbert space for the radiation and the black hole, respectively [12,15]. This relation holds when either $d_R \gg d_B$ or $d_B \gg d_R$. Specifically, $\log d_R$ represents the entropy of the radiation, appropriately regularized up to a certain time, while $\log d_B$ corresponds to the Bekenstein-Hawking entropy of the black hole. Initially, the entropy increases due to the dominance of Hawking saddle, marked by the emission of additional radiation. After the Page time, a shift to the replica wormholes saddle occurs, aligning entropy with the Bekenstein-Hawking value and subsequently declining. This transition guarantees the unitarity of the black hole evaporation process, in accordance with the progression of the Page curve. Notably, similar behavior is observed in the $(3+1)$ -dimensional Reissner-Nordström-AdS black hole, capture the dominant s-wave sector, connected to nongravitational baths within JT gravity [5,6]. This approach applies to almost all black holes [8].

The Lorentzian interpretation of the replica wormholes saddle emphasizes that the entropy $S(R)$ encompasses not only the entropy of quantum field theory (QFT) within the primary region R , but also includes contributions from additional regions behind the black hole horizon, known as entanglement islands [16,17]. These islands exist in the bulk of spacetime, where the metric fluctuates. In the semiclassical limit, the boundary of island, denoted as ∂I , corresponds to the quantum extremal surfaces (QESs), which dynamically extremize the generalized entropy [18–21]

$$S_I(R) = \text{ext}_{\partial I} \left\{ \sum \frac{\text{Area}(\partial I)}{4G_N} + S_{\text{QFT}}(R \cup I) \right\}. \quad (1.3)$$

The QESs can be points in $(1+1)$ D or 2D spatial surfaces in $(3+1)$ D spacetime. The entropy of the primary region R is determined by minimizing over the contributions from the island saddle

$$S(R) = \min_I S_I(R). \quad (1.4)$$

This intricate interplay between entanglement islands and the replica wormholes saddle elucidates the behavior of black hole entropy and its connection to the underlying quantum structure. When the replica wormhole dominates, the island will emerge at the late times, thus the black hole information paradox will be solved hopefully.

Recent research on the black hole information paradox and the Page curve [15,22–33] suggests that isolated regions, or “islands,” emerge during the evaporation of typical black hole models. Additionally, some work has been conducted on phase transitions [34,35]. Observations indicate that phase transitions within the eternal black hole of JT gravity influence the deformation of the Page curve [36–39]. This leads to a deviation from the behavior initially proposed by Page [7], characterized by a straightforward nonmonotonic trend in the black hole entropy.

However, the investigation of the evaporating scenario remains incomplete.

In this paper, we exclude the extremal black hole situation and focus on the entanglement entropy of the nonextremal eternal 4D RN-AdS black hole, following the island rule. Our findings indicate that the island rule resolves the paradox effectively. This outcome is plausible as the entanglement entropy demonstrates that the evaporation process of black hole is unitary and respect with the principles of quantum theory. Subsequently, we investigate the phase transitions specific to the 4D RN-AdS black hole and their influence on the Page curve. In the case of neutrality, the RN-AdS black hole transitions to a 4D Schwarzschild-AdS black hole, where the Hawking-Page phase transition occurs, and the Page curve maintains its standard form. Furthermore, we investigate the Page curve in the context of an eternal black hole to determine how varying charges, Q , influence its structure. Our analysis reveals that as the charge approaches the critical value, Q_c , the effects of the phase transition become less pronounced. We also model the evaporating RN-AdS black hole under the assumption of coupled baths or the removal of the baths to ensure evaporation rather than an eternal black hole state. This approach allows us to observe the Page curve behavior during black hole evaporation. In the charged case, the Page curve displays a variety of behaviors—monotonic, non-monotonic, or even a discontinuity—depending on the event horizon radius. Importantly, these variations do not compromise the unitarity of black hole evaporation.

The structure of this paper is organized as follows: in Sec. II, we provide a brief review of the RN-AdS black hole. In Sec. III, we employ the island formula to compute the entanglement entropy for situation without island and with an island, and then we dedicate to illustrating the Page curve and determining the scrambling time. The effects of phase transitions on the Page curve, influenced by varying the value of charges Q , are explored in Sec. IV. Finally, we presents our conclusions in Sec. V.

II. REVIEW OF RN-ADS BLACK HOLE

We first review some properties of RN-AdS black hole. The RN-AdS black holes in 4D spacetime are characterized by the action in the form of [40]:

$$I = \frac{1}{16\pi G_N} \int d^4x \sqrt{-g} \left(R + \frac{6}{\ell^2} - F_{\mu\nu} F^{\mu\nu} \right), \quad (2.1)$$

where ℓ is the AdS length scale, defined by $\ell \equiv \sqrt{-3\Lambda}$ with Λ being the cosmological constant, R is the Ricci scalar. The metric of 4D static charged RN-AdS black hole is

$$ds^2 = -f(r)dt^2 + \frac{dr^2}{f(r)} + r^2(d\theta^2 + \sin^2\theta d\phi^2). \quad (2.2)$$

Setting the Newton's constant equal to 1, i.e., $G_N = 1$, the function $f(r)$ is defined as follows:

$$f(r) = 1 - \frac{2M}{r} + \frac{Q^2}{r^2} + \frac{r^2}{\ell^2}, \quad (2.3)$$

where M and Q in the metric function are the mass and charge of the black hole, respectively.

One can obtain the Hawking temperature, Bekenstein-Hawking entropy, and the electric potential by deriving the first law, which can be written as follows:

$$\begin{aligned} T &= \frac{1}{4\pi r_+} \left(1 + \frac{3r_+^2}{\ell^2} - \frac{Q^2}{r_+^2} \right), \\ S &= \pi r_+^2, \\ \phi &= \frac{Q}{r_+}. \end{aligned} \quad (2.4)$$

The event horizon is located at $r = r_+$. The mass of the black hole can be derived with the condition $f(r_+) = 0$, i.e.

$$M = \frac{r_+}{2} + \frac{\phi Q}{2} + \frac{r_+^3}{2\ell^2}. \quad (2.5)$$

Clearly, the mass of the black hole is a function of the event horizon radius r_+ , charge Q , and electric potential ϕ .

In AdS spacetime, an infinitely large effective potential exists at the boundary of spacelike infinity. This potential reflects the Hawking radiation emitted by AdS black holes back toward them, effectively transforming the AdS spacetime into an infinite potential well. In the case of AdS black holes with sufficiently large mass, the reflected Hawking radiation can return to the black hole rapidly enough to establish a thermal equilibrium. This results in a stable black hole with a nonzero temperature that does not undergo evaporation. To induce evaporation in the black hole, we introduce a coupling with a nongravitational bath at finite temperature, as described by Almheiri *et al.* in [9]. Our study focuses on an AdS black hole that has reached equilibrium with a bath located at the boundary, making the black hole evaporate. One can refer to Fig. 1.

Then the black hole could evaporate in this way. In order to obtain the maximally extended double-sided geometry and to better facilitate subsequent calculations, we perform the Kruskal coordinate transformation. The definition of the tortoise coordinate is

$$r_*(r) = \int^r \frac{1}{f(r)} dr, \quad (2.6)$$

and the Kruskal coordinates are defined as

$$U = -e^{-\kappa(t-r_*)}, \quad V = +e^{\kappa(t+r_*)}, \quad (2.7)$$

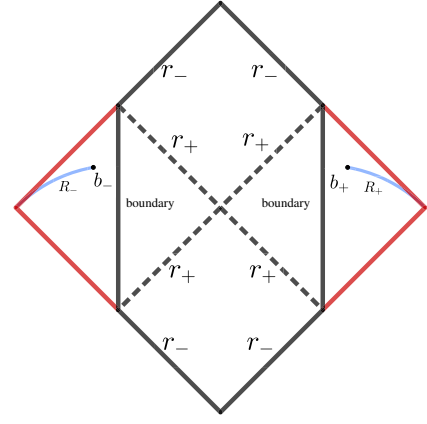


FIG. 1. The Penrose diagram of an eternal 4D RN-AdS₄ black hole without island. The black region represents the black hole, and the red region denotes the bath region. The boundary conditions are imposed on the boundary. R_{\pm} indicate the radiation regions on the right and left wedges, and b_{\pm} are the boundaries of the radiation regions R_{\pm} .

where κ is the surface gravity, which can be written as

$$\kappa = \frac{1}{r_+^2} \left(M - \frac{Q}{r_+} \right) + \frac{r_+}{\ell^2}. \quad (2.8)$$

We refer to the Kruskal-Szekeres coordinate in the RN-AdS spacetime which is given by

$$\begin{aligned} ds^2 &= -\Omega^2(r) dU dV \\ &= -\Omega^2(r) \kappa^2 e^{2\kappa r_*} dt^2 + \Omega^2(r) \kappa^2 e^{2\kappa r_*} f^{-2}(r) dr^2, \end{aligned} \quad (2.9)$$

comparing Eqs. (2.3) and (2.9), we obtain the conformal factor $\Omega(r)$ in bulk spacetime¹

$$\begin{aligned} \Omega^2(r) &= \frac{1}{\kappa^2 e^{2\kappa r_*}} f(r) \\ &= \frac{(-Q + Mr_+ + r^4)(Q^2 + r(-2M + r + r^3))}{r^5}. \end{aligned} \quad (2.10)$$

Due to the fact that bath is in a Minkowski spacetime, characterized by the metric $ds^2 = -dt^2 + dr^2$, in the flat thermal bath region, this conformal factor is

$$\Omega^2(r) = \frac{1}{\kappa^2 e^{\kappa r}}. \quad (2.11)$$

In this way, the black hole is able to radiate, allowing the asymptotic observer to collect Hawking radiation in the bath region. Consequently, the island formula can be employed to calculate the entanglement entropy of the Hawking radiation.

¹After here, we set the AdS length $\ell = 1$ for convenience.

III. ENTANGLEMENT ENTROPY IN 4-DIMENSIONAL RN-ADS BLACK HOLE

In this section, we calculate the entanglement entropy of a 4D RN-AdS black hole in two different situation: one without island, and the other with island during the black hole's late-stage evaporation. The island formula is given by

$$S(R) = \min \left\{ \text{ext} \left[\frac{\text{Area}(\partial I)}{4G_N} + S_{\text{Bulk}}(R \cup I) \right] \right\}. \quad (3.1)$$

For simplicity, we only consider the single island case, as multiple islands contribute only to sub-leading terms and do not affect our main results. Consequently, our analysis will concentrate on the emergence of a single island at the final stage of evaporation.

A. Without island

First, we calculate the entanglement entropy without an island at early times. Due to the divergent nature of entropy in higher dimensions, and the absence of a definitive formula for its calculation, we adopt a large distance limit to validate the s-wave approximation which neglect the spherical part of the metric and only considers the conformally flat part. Thus, the Hawking radiation can be described properly by a long distance observer. In this paper, we exclusively focus on the neutral uncharged radiation from the black hole and disregard the Schwinger effect. This configuration is shown in Fig. 1.

We assume that the entire system is in a pure state at $t = 0$. We set the coordinates of these two points are $(t, r) = (t_b, b)$ and $(-t_b - i\beta/2, r) = (t_b, b)$, respectively. According to the complementarity principle of von Neumann entropy, the entropy of the conformal field theory (CFT) in the region outside $(-\infty, b_-) \cup (b_+, +\infty)$ is equivalent to the entropy of the radiation region. Correspondingly, the entanglement entropy of the radiation is given by

$$S_{\text{Bulk}} = S(R) = \frac{c}{3} \log[d(b_+, b_-)]. \quad (3.2)$$

where c is the central charge. The $d(b_+, b_-)$ is the geodesic distance between the point b_{\pm} . Then, we have

$$\begin{aligned} d(b_+, b_-)^2 &= \Omega(b_+) \Omega(b_-) [U(b_-) - U(b_+)] \\ &\quad \times [V(b_+) - V(b_-)] \\ &= \Omega^2(b) [U(b_-) - U(b_+)] [V(b_+) - V(b_-)], \end{aligned} \quad (3.3)$$

where the conformal factor $\Omega^2(b)$ could be written as (2.11)

$$\Omega^2(b) = \frac{1}{\kappa^2 e^{2\kappa b}}. \quad (3.4)$$

Therefore, the entanglement entropy without island is given by

$$\begin{aligned} S_{\text{Rad}} &= \frac{c}{6} \log \left[\frac{1}{\kappa^2 e^{2\kappa b}} 2e^{2\kappa b} [\cosh(2\kappa t_b) + 1] \right] \\ &= \frac{c}{6} \log \left[\frac{4}{\kappa^2} [\cosh^2(\kappa t_b)] \right]. \end{aligned} \quad (3.5)$$

For late times ($t_b \rightarrow \infty$), the above equation simplifies to

$$\begin{aligned} S_{\text{Rad}} &\simeq \frac{c}{6} \log \left(\frac{4}{\kappa^2} \frac{1}{4} e^{2\kappa t_b} \right) = \frac{c}{6} \log \left(\frac{1}{\kappa^2} e^{2\kappa t_b} \right) \\ &\simeq \frac{c}{3} \kappa t_b, \end{aligned} \quad (3.6)$$

which exhibits linear growth in time. Therefore, at late times, the entropy of radiation will exceed the Bekenstein-Hawking entropy of the black hole, leading to eventual loss of information from the black hole due to the absence of an S matrix that ensures unitary evaporation. Such a situation presents a contradiction with the finite von Neumann entropy of a finite-dimensional black hole system, implying that the black hole would evolve to a mixed state, thereby violating the principle of unitarity. It shapes the enigma known as the black hole information paradox. To solve this issue, we propose the inclusion of an island in our subsequent calculations. We expect that the emergence of an island could resolve these inconsistencies and restore unitarity in black hole evaporation.

B. With island

In the subsequent analysis, we consider another modified gravitational method, i.e., the proposal of quantum entanglement islands. Although entanglement entropy generally depends on the cutoff surface² scale, in 2D systems with conformal symmetry, one can employ regularization and renormalization techniques to obtain a well-defined entanglement entropy. This approach was pioneered by Holzhey, Larsen, and Wilczek [41], and later refined by Bianchi and Smerlak [42]. From this, we can derive the formula for fine-grained entropy. We calculate the entanglement entropy with an island at the late stage of black hole evaporation. The entanglement entropy for this disconnected interval $R \cup I$ (see Fig. 2) as follows [23]:

$$S_{\text{bulk}}(R \cup I) = \frac{c}{3} \log \frac{d(a_+, a_-) d(b_+, b_-) d(a_+, b_+) d(a_-, b_-)}{d(a_+, b_-) d(a_-, b_+)}. \quad (3.7)$$

²The cutoff surface is artificially selected, and it is generally stipulated that Hawking radiation is emitted from the cutoff surface by considering the back-reaction of radiation. For a 4D Schwarzschild black hole, the cutoff surface is approximately 2–3 times of the Schwarzschild radius, a region where gravitational effects can be considered negligible.

We define the coordinates of the island as $a_{\pm} = (\pm t_a, a)$. Using the Kruskal coordinates and applying the conformal factor $\Omega(r)$, the generalized entanglement entropy in this time is

$$S_{\text{gen}} = \frac{2\pi a^2}{G_N} + \frac{c}{6} \log \left[\frac{16f(a)}{\kappa^4} \cosh^2(\kappa t_a) \cosh^2(\kappa t_b) \right] + \frac{c}{3} \log \left[\frac{\cosh[\kappa(r_*(a) - r_*(b))] - \cosh[\kappa(t_a - t_b)]}{\cosh[\kappa(r_*(a) - r_*(b))] + \cosh[\kappa(t_a + t_b)]} \right]. \quad (3.8)$$

First, we consider the behavior of entanglement entropy at early times. We assume that the following approximation is valid

$$t_a, t_b \simeq 0, \quad t_a, t_b \ll r_+, \quad t_a, t_b \ll 1/\kappa \ll r_*(b) - r_*(a). \quad (3.9)$$

We pick the cutoff surface far away from the horizon $b \gg r_+$. Then the last term in the generalized entropy can be properly omitted in this approximation. The generalized entropy is given approximately as follows

$$S_{\text{gen}}(\text{early}) \simeq \frac{2\pi a^2}{G_N} + \frac{c}{6} \log \left[\frac{16f(a)}{\kappa^4} \cosh^2(\kappa t_a) \cosh^2(\kappa t_b) \right] \simeq \frac{2\pi a^2}{G_N} + \frac{c}{6} [\log f(a) + \cosh(2\kappa t_a)]. \quad (3.10)$$

In order to obtain the location of the island, we need to solve the following equation. By extremizing the generalized entropy

$$\frac{\partial S_{\text{gen}}(\text{early})}{\partial t_a} = \frac{c\kappa}{3} \tanh(\kappa t_a) = 0, \quad \frac{\partial S_{\text{gen}}(\text{early})}{\partial a} = \frac{4\pi a}{G_N} + \frac{c}{6} \frac{f'(a)}{f(a)} = 0. \quad (3.11)$$

The solution to the first equation is $t = 0$. For the second equation, employing approximation methods and assuming the higher-order terms of $\frac{a-r_+}{r_+}$ to be negligible, we deduce an effective solution $a \simeq r_+$ plus higher-order terms, which are smaller than the Planck length l_p . This result suggests that there is no quantum extremal surface that leads to the

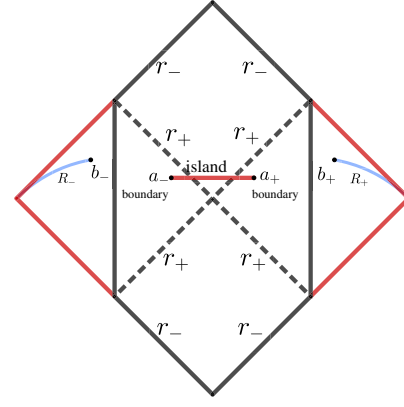


FIG. 2. The Penrose diagram of an eternal 4D RN-AdS black hole with an island. R_{\pm} are the radiation regions on the right and left wedges, and b_{\pm} are the boundaries of the radiation region R_{\pm} . The boundary of the island is denoted as a_{\pm} .

increase of entropy to the extremal point before the Page time. The entanglement entropy of the radiation only relies on the radiation itself in the early time and is not affected by the island. Subsequently, we extend our analysis at late times situation where an island emerges.

Now we turn to the construction with a single island. In this time, the construction of the matter entropy also grows, exhibiting a linear increase in fine-grained entropy during the late stages of black hole evaporation. This phenomenon is expected to occur around the Page time. There are some approximate equations as follows

$$t_a, t_b \gg b > r_+, \quad \cosh(\kappa t) = (e^{\kappa t} + e^{-\kappa t})/2, \quad \cosh \kappa_+(t_a + t_b) \gg \cosh \kappa_+(r_*(a) - r_*(b)), \quad \cosh \kappa_+(r_*(a) - r_*(b)) \simeq \frac{1}{2} e^{\kappa_+(r_*(b) - r_*(a))}. \quad (3.12)$$

Thus the distance among the points, a_{\pm} and b_{\pm} will have following behavior as [23]

$$d(a_+, a_-) \simeq d(b_+, b_-) \simeq d(a_+, b_-) \simeq d(a_-, b_+) \geq d(a_+, b_+) \simeq d(a_-, b_-). \quad (3.13)$$

Plugging Eq. (3.13) into Eq. (3.8), the generalized entropy is given by

$$S_{\text{gen}}(\text{late}) = \frac{2\pi a^2}{G_N} + \frac{c}{6} \log \left[\frac{16f(a)}{\kappa^4} \cosh^2(\kappa t_a) \cosh^2(\kappa t_b) \right] + \frac{c}{3} \log \left[\frac{\cosh[\kappa(r_*(a) - r_*(b))] - \cosh[\kappa(t_a - t_b)]}{\cosh[\kappa(r_*(a) - r_*(b))] + \cosh[\kappa(t_a + t_b)]} \right] \simeq \frac{2\pi a^2}{G_N} + \frac{c}{3} \log \left[\frac{4\sqrt{f(a)}}{\kappa^2} [\cosh[\kappa(r_*(b) - r_*(a))] - \cosh[\kappa(t_a - t_b)]] \right] \simeq \frac{2\pi a^2}{G_N} + \frac{c}{3} \log \left[\frac{4\sqrt{f(a)}}{\kappa^2} \right] - \frac{c}{3} (r_*(a) - b) - \frac{2c}{3} e^{-\kappa(b - r_*(a))}, \quad (3.14)$$

where in the second approximate equation, we take the partial derivative of S with respect to t

$$\frac{\partial S_{\text{gen}}(\text{late})}{\partial t_a} = \frac{c}{3} \frac{\kappa \sinh \kappa(t_a - t_b)}{\cosh[\kappa(r_*(a) - r_*(b))] - \cosh[\kappa(t_a - t_b)]} = 0. \quad (3.15)$$

We find that the partial derivative equation (3.15) is equal to zero only when $t_a \approx t_b$, which implies that the generalized entropy is independent of time. By solving the extremal condition $\partial S_{\text{gen}}/\partial a = 0$, we obtain

$$\frac{4\pi a}{G_N} = \frac{c}{3f(a)} [2\kappa e^{-\kappa(r_*(b) - r_*(a))} + 1] - \frac{c f'(a)}{6f(a)}. \quad (3.16)$$

At late times and in the large distances limit (3.13), we can take the near horizon limit, $a \simeq r_+$. We can approximate the tortoise coordinate r_* by

$$\begin{aligned} f(r) &\simeq f'(r)(r - r_+) = 2\kappa(r - r_+), \\ r^*(r) &= \int \frac{1}{f(r)} dr \simeq \frac{1}{2\kappa} \int \frac{dr}{r - r_+} \\ &= \frac{1}{2\kappa} \log \left| \frac{r - r_+}{r_+} \right|. \end{aligned} \quad (3.17)$$

Substituting the approximation into Eq. (3.16), we obtain the following result

$$a = \frac{c}{4\pi G_N} \left(\frac{1}{2} - \frac{1}{2} \sqrt{1 - \frac{8\pi G_N r_+}{c^2} \left(1 + \frac{c}{6r} (e^{-b\kappa} + 1) \right)} \right) \quad (3.18)$$

Performing a Taylor expansion, we obtain the final expression

$$a \simeq r_+ + \frac{c^2 G_N^2}{12^2 \pi r_+^3} e^{-2\kappa b} + \mathcal{O}(G_N^3). \quad (3.19)$$

By analyzing the expression, we can derive the entanglement entropy

$$\begin{aligned} S &= \frac{2\pi r_+^2}{G_N} + \mathcal{O}(G_N^3) \\ &\simeq 2S_{\text{BH}}. \end{aligned} \quad (3.20)$$

The second term has a finite value. Therefore, at late times, the dominant contribution to entanglement entropy is provided by the Bekenstein-Hawking entropy. The entanglement entropy of an eternal black hole will remain constant during its evaporation, ensuring the unitarity of the final state. This approach is more reasonable and addresses our problem in the result (3.6) in the final step. Consequently, the island solution is consistent with the Page curve prediction, indicating that

Hawking radiation is unitary and information is preserved in the 4D RN-AdS black hole.

C. Page curve and scrambling time

In this section, we calculate the Page time and scrambling time. Based on the value of entanglement entropy at early times and late times, we can plot the Page curve.

Page time is the time when entropy grows to its maximal value. At early times, the dominant term is as shown in equation (3.6), while later, the term in equation (3.20) becomes larger than the time-dependent term. We estimate the Page time by identifying the point of intersection between the entropy curve without the island at very early times and the entropy curve with the island at late times. We determine the Page time by equating Eqs. (3.6) and (3.20). Letting them be nearly equal during the late times and using the Hawking temperature $T_H = \frac{\kappa}{2\pi}$, we can perform the calculation as follows

$$\begin{aligned} t_{\text{Page}} &\simeq \frac{6S_{\text{BH}}}{c\kappa} \\ &\simeq \frac{3S_{\text{BH}}}{c\pi T_H}. \end{aligned} \quad (3.21)$$

According the location of island, we find that the island emerges near the horizon. Then, we obtain the Page curve as shown in Fig. 3.

The scrambling time is the shortest time for an outside observer to recover the information in the Hawking radiation that fell into the black hole before [24,43]. It approximate through Eqs. (3.17) and (3.19), and is given by

$$\begin{aligned} t_{\text{scr}} &\equiv \text{Min}[\Delta t] = r_*(b) - r_*(a) \\ &= b - \frac{1}{2\kappa} \log \left| \frac{c^2 G_N^2}{144 \times 4\pi r_+^4} e^{-2\kappa b} \right| \\ &\simeq \frac{1}{\kappa} \log \left(\frac{12 \times 2\pi r_+^2}{c G_N e^{-\kappa b}} \right) \\ &\simeq \frac{1}{\kappa} \log S_{\text{BH}}, \end{aligned} \quad (3.22)$$

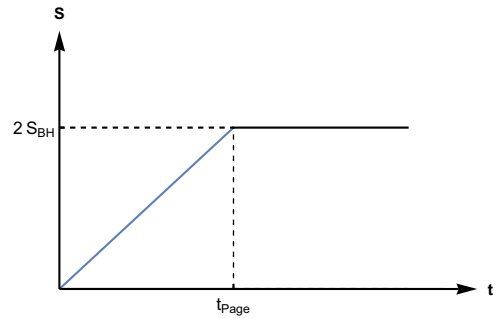


FIG. 3. Page curve of 4D RN-AdS black hole. The blue line represents entanglement entropy at the early times, while the black line represents entropy at late times. They intersect at the point in $2S_{\text{BH}}$ at time t_{Page} .

where we have used the Eq. (3.19) to reduce, and use the near horizon approximation, and r_+ is much larger than other terms, so the logarithm of r_+ is almost the same as r_+ in the third line.

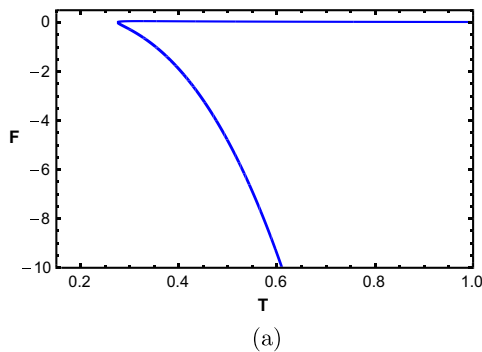
IV. PHASE TRANSITIONS AND PAGE CURVE

In our previous discussions, we have analyzed the situations both without island and with an island in the context of entanglement entropy. Our next objective is to investigate the possibility of a first-order phase transition occurring in the RN-AdS black hole, a phenomenon that could potentially influence the entanglement entropy of evaporating black hole. This consideration is integral to our analysis, and henceforth, this section is dedicated to examining the Page curve as affected by the phase transitions of the black hole.

Initially, we ascertain the phase transition by evaluating the free energy of the RN-AdS black hole. The free energy \mathcal{F} can be obtained by computing the Euclidean action in the semiclassical approximation, and it is given by

$$\begin{aligned}\mathcal{F}(T, V) &= M - TS \\ &= \frac{1}{2} \left(r_+ - 2\pi T r_+^2 + \frac{Q^2}{r_+} \right).\end{aligned}\quad (4.1)$$

Subsequently, we plot the $\mathcal{F} - T$ diagram, referenced in Fig. 4(a), and compare it to the temperature-radius $T - r_+$ diagram, as detailed in Fig. 4(b). It becomes conspicuously evident that in the $Q = 0$ case, only the Hawking-Page phase transition occurs. This phenomenon signifies that a black hole with larger free energy is more unstable. Consequently, in such a case, only a solitary black hole exists. Therefore, when the charge $Q = 0$, the Page curve is unaffected by the Hawking-Page first-order phase transition, as shown in Fig. 5.



Further, we present the $T - r_+$ diagram and the $\mathcal{F} - T$ diagram, as depicted in Fig. 6, for the $Q \neq 0$ case. Here, we consider eternal black holes with varying charges Q . It becomes evident that as the charge Q approaches the critical charge, which permits phase transitions, its impact on the Page curve nearly diminishes. Delving deeper into this effect, we focus on the most pronounced case where the charge Q is small.

Drawing inspiration from the aforementioned results, we simulate the evaporation of the RN-AdS black hole under scenarios involving coupled baths or the absence thereof. This allows us to determine the effects on the evaporating black hole, particularly how these different conditions influence the black hole's temperature, entropy, and the Page curve. By comparing these cases, we aim to deepen our understanding of black hole thermodynamics and information preservation during the evaporation process. Additionally, we discuss whether phase transitions occurring before or after the Page time induce any alterations in the Page curve. We uncover an intriguing phenomenon—the behavior of the Page curve, whether monotonic, non-monotonic, or discontinuous, is predicated on the initial event horizon radius r_+ . The intricate details of this analysis are delineated in the following subsection.

A. Neutral case

First, we observe the case where the charge $Q = 0$, reducing the RN-AdS black hole to a Schwarzschild-AdS black hole. The 4D Schwarzschild black hole has only one horizon, labeled as r_+ . The free energy is given by

$$\mathcal{F} = \frac{1}{2} (r_+ - 2\pi T r_+^2), \quad (4.2)$$

and the temperature can be written as

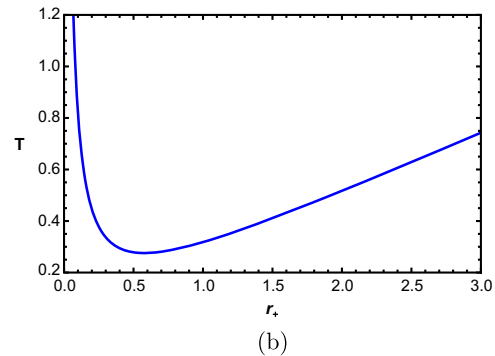


FIG. 4. The $\mathcal{F} - T$ figure for Schwarzschild black holes. (a) On the left, for $Q = 0$, the $T - \mathcal{F}$ Figure. \mathcal{F} is depicted as functions of T when $Q = 0$. As r_+ increases, the temperature corresponds to two distinct values of free energy within the range $0.276 < T < 0.609$. This implies the presence of only one black hole in this case, as the branch with the lower free energy is more stable. (b) On the right, for $Q = 0$, the $T - r_+$ diagram. Each r_+ corresponds to a unique temperature T . T is a function of r_+ , and as r_+ becomes large, the temperature also increases significantly.

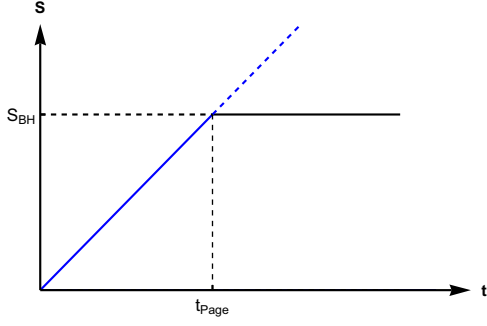


FIG. 5. Page curve of 4D Schwarzschild black hole. The Page curve is delineated by a blue line representing the entanglement entropy in the early stages, and a black line indicating the entropy at later stages. These lines intersect at a point designated as S_{BH} , corresponding to the pivotal time t_{Page} . Notably, this convergence is unaffected by the Hawking-Page phase transition.

$$T = \frac{1}{4\pi r_+} (1 + 3r_+^2). \quad (4.3)$$

According to [44,45], a Hawking-Page phase transition occurs between an AdS black hole with radiation and thermal AdS. To illustrate this, we can depict the free energy, \mathcal{F} , as a function of the temperature T , and similarly, the radius r_+ as a function of the temperature T . As illustrated in Fig. 4, when the black hole temperature $T > 0.276$, at the fixed temperature, there are two primary classifications of black holes based on size. The $\mathcal{F} - T$ curve shows that there are two values of free energy at the same temperature. This indicates that there exists only one more stable black hole with a larger black hole radius, because when the temperature is fixed, the lower free energy, which is related to the black hole, is more stable.

The entanglement entropy of the Schwarzschild black hole can be computed using Eq. (3.1), analogous to the method delineated in Sec. III. Drawing parallels to the

RN-AdS black hole, the equation governing the parameter retains the identical form as presented in Eqs. (3.18) and (3.19). The resultant entanglement entropy is articulated as

$$S_{\text{Sch}} = \text{Min} \left[\frac{2}{3} \pi T(r_h) t, \frac{4\pi r_+^2}{G_N} \right]. \quad (4.4)$$

The Page curve, as depicted in Fig. 5, initially increases linearly and tends to level off after the Page time.

B. Charged case

In this charged case, we leverage the analogy between the RN-AdS black hole and the van der Waals fluid, as established in Ref. [46], especially in the context of phase transitions. We examine how the Page curve is altered by varying the event horizon radius r_+ .

Firstly, we plot the free energy \mathcal{F} as a function of temperature T , as shown in Fig. 6(a). The $\mathcal{F} - T$ curves, colored blue and orange, display the characteristic swallowtail behavior when the charge Q is below a certain value of charge, which is a candidate of the value of critical charge Q_c . Conversely, scenarios where Q equals to or exceeds this certain value of charge are represented by smooth curves, depicted in red or green. This diagram indicates that a phase transition occurs for $0 < Q < Q_c$, with the critical point being an inflection point. For $Q > Q_c$, it represents a thermodynamically stable branch with no phase transition structures. The blue and orange curves each have three branches: the lower branch corresponds to the large black hole (LBH), the upper branch to the small black hole (SBH), and the other branch means there is an intermediate black hole. The intersection point of these branches marks the critical point of the phase transition. Below the critical temperature, the LBH is more stable with lower free energy, and vice versa. The phase transition occurs as the temperature crosses this critical value.

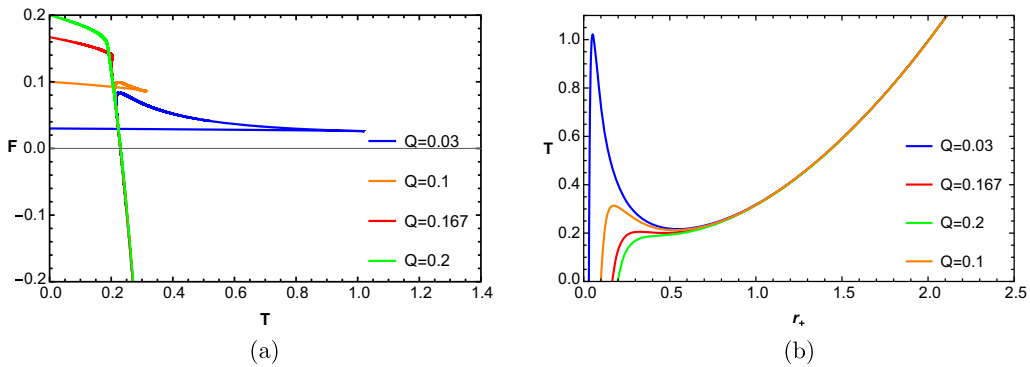


FIG. 6. (a) The diagram for free energy \mathcal{F} and temperature T with nonvanishing charges. Here we set the charge smaller or larger than Q_c , as well as equal to the critical charge. When $Q < Q_c$, the $\mathcal{F} - T$ curve shows the characteristic swallowtail behavior, indicating an impending phase transition. Conversely, for $Q > Q_c$, the $\mathcal{F} - T$ curve remains smooth. (b) On the right, the $T - r_+$ figure with $Q = 0.03, 0.01, 0.167$, and 0.2 . At low temperatures, only one black hole exists. As the temperature increases and $Q < Q_c$, three distinct black holes emerge; however, due to the instability of the intermediate black hole, only a large and a small black hole remain; when $Q > Q_c$, there is no phase transition.

As indicated by the blue and orange line in Fig. 6(b), there is a black hole phase transition. However, for the $Q > Q_c$ case, no phase transition is observed, as shown by the red and green lines. In the case of $Q < Q_c$, the size of black hole gradually increases with temperature until a critical point is reached, where two new black holes coexist with the existing black hole. As the temperature increases, one of these new black holes diminishes in size, while the other expands. These two black holes persist up to a certain temperature, beyond which the smaller and intermediate black holes coalesce and disappear, leaving only a large black hole at elevated temperatures. The occurrence of a phase transition precipitates a sudden shift in entanglement entropy, thereby changing both the form of Page curve and the Page time.

Then, we calculate the value of critical charge and the critical event horizon radius. To find these parameters, we take the partial derivative of the temperature equation

$$\frac{dT}{dr_+} = \frac{1}{4\pi} \left(-\frac{1}{r_+^2} + 3 + \frac{3Q^2}{r_+^4} \right), \quad (4.5)$$

and make the temperature equation to be second-order derivative

$$\frac{d^2T}{dr_+^2} = \frac{1}{2\pi r_+^3} - \frac{3Q^2}{\pi r_+^5}. \quad (4.6)$$

Setting the equation to zero allows us to establish the relationship $r_{+c} = \sqrt{6}Q_c$, from which we can deduce the critical electric charge $Q_c = 0.167$. Consequently, we calculate the critical temperature T_c , which corresponds to the abscissa at the intersection point of the curves in Fig. 6(a). This critical point demarcates the boundary between different thermodynamic behaviors of the black hole.

In the aspect of thermodynamics, the black hole phase transition can be compared with the van der Waals first order phase transition mentioned before in [46]. We plot the Fig. 6(b) again, which added an “isobar” and delineating three different value of Q curves as Fig. 7 shows. In the real evaporation process, for instance, the “oscillating” part will be replaced by the part of red dotted line which corresponds to the temperature T_0 determined using the Maxwell equal area rule, in Fig. 7 when $Q = 0.03$, and the critical charge is $Q_c = 0.167$. As previously mentioned, the radius of black hole from r_1 to r_3 is unstable. The entanglement entropy will be elucidated as follows

$$S = \text{Min} \left[\frac{2}{3} \pi T(r_+) t, 2S_{\text{BH}} \right], \quad (4.7)$$

where $T(r_+)$ is defined by

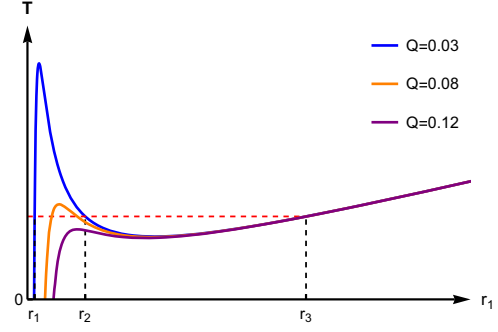


FIG. 7. The $T - r_+$ diagram with $Q = 0.03$, $Q = 0.08$ and $Q = 0.12$. There is only one black hole in the low temperature. As the temperature rises, the instability of the intermediate black hole leads to the existence of two distinct black holes.

$$T(r_+) = \begin{cases} \frac{1}{6r_+} \left(1 + 3r_+^2 - \frac{Q^2}{r_+^2} \right), & \text{if } 0 < r_+ < r_1 \\ T_0, & \text{if } r_1 < r_+ < r_3 \\ \frac{1}{6r_+} \left(1 + 3r_+^2 - \frac{Q^2}{r_+^2} \right), & \text{if } r_+ > r_3 \end{cases} \quad (4.8)$$

Besides, the Page time varies with temperature. As the radius r_+ increases linearly, the Page time can be approximated by the following relationship

$$t_{\text{Page}} \simeq \frac{3S_{\text{BH}}}{c\pi T(r_+)}. \quad (4.9)$$

It is intriguing to examine the correlation between phase transition and Page time. The occurrence of a phase transition either before or after the Page time may influence the Page curve. This will be the subject of further discussion.

In our study, we focus exclusively on the case where $Q < Q_c$ to investigate the impact of phase transitions. In the context of nonextremal eternal black holes, we consider three specific charge values: $Q = 0.03$, $Q = 0.08$, and $Q = 0.1$. By substituting these values into the Eq. (4.7), we can construct 3D Page curves. These curves are characterized by coordinates representing the event horizon radius of black hole r_+ , time t , and generalized entropy S . Analyzing these diagrams, one can observe that as the charge Q decreases, the phenomenon of phase transition becomes more pronounced, which also as Fig. 9(a) shows. There are jumps between $r_+ > r_{+c}$ and $r_+ < r_{+c}$ which promise the phase transition to happen. When the event horizon radius r_+ is smaller than the critical value r_{+c} , the Page time exhibits a dependence on the charge Q . Specifically, it appears as a concave curve in the middle portions of the figures shown in Fig. 8. In the case of small r_+ (as depicted in Fig. 7 for $r_+ < r_1$), the Page time occurs relatively early as Fig. 9(a) blue line shows. However, as r_+ increases (corresponding to intermediate-sized black

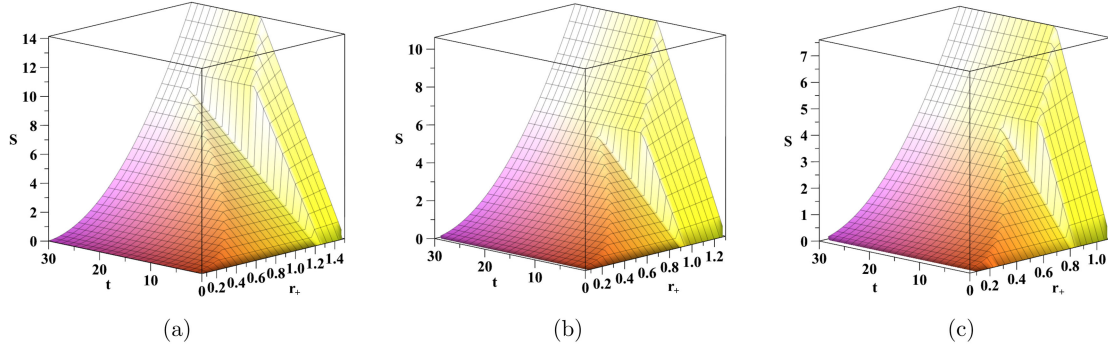


FIG. 8. The Page curves of eternal RN-AdS black hole. (a) Page curves for the charged $Q = 0.03$ case. (b) Page curves for the charged $Q = 0.08$ case. (c) Page curves for the charged $Q = 0.1$ case.

holes), the Page time shifts with r_+ . Interestingly, for LBH, the Page time remains smaller than that of intermediate black holes but larger SBH case as shown in Fig. 9(b). Conversely, when r_+ exceeds the critical value r_{+c} , the generalized entropy corresponding to the Page curve increases with r_+ [as described by (4.7)]. Furthermore, at a fixed radius, smaller charge values lead to shorter Page times, as shown in Fig. 9(c). Clearly, the charge Q significantly influences both the Page time and the occurrence of phase transitions. Remarkably, we find that as the charge Q decreases further, the impact on phase transitions becomes even more pronounced.

Moving forward, we draw inspiration from previous works such as [9,47–49]. Specifically, we explore the concept of coupling between one boundary and an external auxiliary system (acting as a heat sink). This coupling allows a two-sided black hole to undergo evaporation on one side. In the case of coupled baths, the black hole is allowed to exchange energy with its surroundings, leading to a gradual decrease in mass. The exchange process is assumed not to be influenced by the charge of black hole. As the black hole evaporates, its temperature and entropy undergo significant changes, which are reflected in the Page curve's behavior. Conversely, the removal of thermal baths isolates the black

hole, causing it to follow a different evaporation trajectory. Without the energy exchange, the black hole's temperature rises sharply, accelerating the evaporation process. This rapid change can lead to a more pronounced effect on the Page curve, potentially resulting in a steeper decline or even discontinuities. Now we take it into consideration.

During the black hole's evaporation process, its event horizon radius r_+ evolves with time. According to Refs. [50,51], the rate of change of r_+ with respect to time $dr_+/dt = -x$ is governed by a constant denoted as x . This constant incorporates fundamental physical quantities such as \hbar , c , G , and M .

For simplicity and clarity, we set the charge $Q = 0.03$, ensuring that it remains smaller than the critical charge Q_c . This choice guarantees the occurrence of a phase transition during the process. The subsequent work discusses the Page curve structure for different ranges of the event horizon radius: $r > r_3$, $r_1 < r < r_3$, and $r < r_1$. The Page curve diagrams corresponding to these three distinct event horizon scenarios are presented in Fig. 10.

Figure 10(a) shows that the Page curve initially increases in the early times. However, in the time half past the evaporation time, the Page curve for the LBH, where $r_+ > r_1$, exhibits a discontinuity. Subsequently, the curve

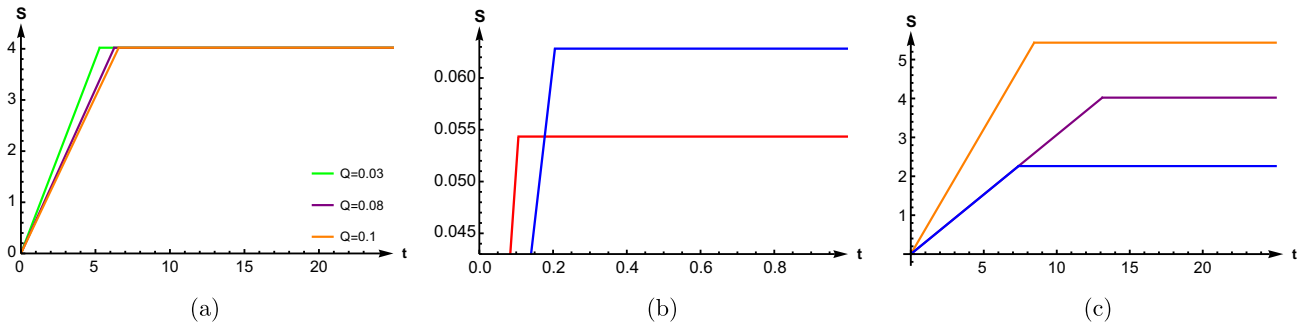


FIG. 9. The Page curves of eternal RN-AdS black hole. (a) Page curves for the charge $Q = 0.03$, $Q = 0.08$ and $Q = 0.1$ cases, respectively. (b) Page curves for the charge $Q = 0.08$. SBH with the red line, while intermediate black hole case with the blue line. (c) Page curves for the charge $Q = 0.08$ case. Intermediate black hole case with purple and blue lines, and the LBH case with an orange line.

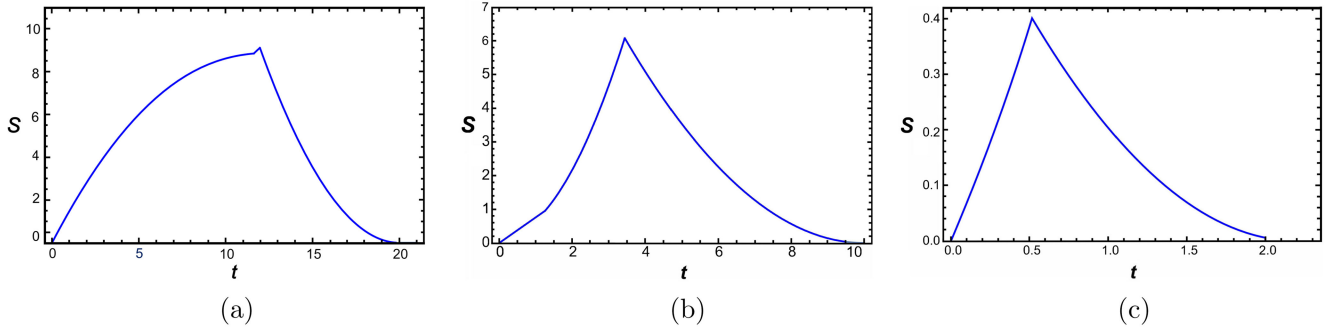


FIG. 10. The Page curve of a 4D RN-AdS black hole initially coupled to a bath, then isolated to allow for evaporation. (a) The Page curve for an RN-AdS black hole with a large horizon radius, where $r_+ > r_1$, as shown in Fig. 7. (b) The Page curve for an RN-AdS black hole with an intermediate event horizon radius. (c) The Page curve for a small RN-AdS black hole.

trends downward until the entropy reaches zero. If we assume the event horizon radius decreases linearly over time, the entanglement entropy reaches a minimum, and the Bekenstein-Hawking entropy term is depicted as a three-segment piecewise function. This configuration results in a Page curve that encapsulates the effects of the Hawking-Page phase transition, with the discontinuity arising from the phase transition itself.

Figure 10(b) demonstrates that for the intermediate black hole, which lies between r_1 and r_2 in Fig. 7, the Page curve initially increases linearly. However, at the beginning of the evaporation, the discontinuity becomes more pronounced than in the Page curve of the large black hole. As with the larger black hole case, the form of the evaporating black hole is time-dependent. The Bekenstein-Hawking entropy term is modeled as a two-segment piecewise function, leading to an overall entropy that starts by following the minimal value of temperature times time t and then shifts to a constant value, signaling a phase transition. This suggests that the unstable black hole transitions into a smaller black hole before the phase transition. The sharp change in temperature as the black hole's phase shifts causes the slope changes, indicating that if the phase transition occurs before the Page time, the Page curve will exhibit a notable deviation.

Figure 10(c) depicts the Page curve of SBH is monotonically increasing, but it declines after the Page time. At late stage time of the process, the entanglement entropy turns into zero suddenly. In the final stages of the evaporation process, the entanglement entropy abruptly reduces to zero. As depicted in Fig. 7, the absence of a phase transition maintains the Page curve in its canonical form. Consequently, the Page curve for a small black hole does not reflect any phase transition. Notably, for minuscule radii, the Page time exhibits an increase over time in contrast to that of a larger black hole, attributable to the negative heat capacity.

V. DISCUSSION AND CONCLUSION

We study the Page curve of Reissner-Nordström AdS black holes in 4D spacetime under a variety of conditions,

by using the island formula (3.1). Initially, we introduce couplings to the bath, enabling Hawking radiation to reach null infinity and initiating the evaporation of the RN-AdS black hole. In scenarios without island, entropy escalates indefinitely over time, as delineated in Eq. (3.6), contradicting the Bekenstein-Hawking entropy bound and violating the unitarity principle of quantum mechanics. To resolve this paradox, we integrate the concept of an entanglement island in the RN-AdS black hole framework. Our subsequent analysis of the process involving an island reveals that multiple islands yield a smoother Page curve compared to the single island case. According to the island formula, after the Page time, the Bekenstein-Hawking entropy is the predominant term. After the Page time, the entanglement entropy stabilizes at a constant value due to the emergence of islands, as calculated in Eq. (3.20), reflecting the behavior of an evaporating black hole. The Page curve depicting the evaporation process of the eternal black hole is illustrated in Fig. 3.

Next, we explore the impact of the charged parameter Q on the Page curve when $Q < Q_c$. Specifically, we plot the Page curve for the eternal 4D RN-AdS black hole, as shown in Fig. 8. Remarkably, we observe that as the charge Q decreases, the effects on the Page curve become more pronounced, as shown in Fig. 9(b). During phase transitions, the early stages of Hawking radiation entropy exhibit significant changes. In the context of replica wormholes, the transition from the Hawking saddle to the replica wormholes saddle involves additional time, which indicated in the Fig. 8, where the curve spends more time reaching to Page time. However, when no phase transition occurs, the Page curve aligns with the original proposal by Page, where the generalized entropy depends on the value of the event horizon radius r_+ . We note that the charge factor becomes pivotal when a charged black hole evaporates.

We assume that the radius monotonically decreases over time, implying that Hawking radiation does not deplete the black hole's charge, thus maintaining a constant charge throughout the process. Through an examination of the

island configuration and phase transitions, we investigate information preservation in 4D RN-AdS black holes, focusing on the effects of phase transition on the Page curve across various black hole sizes. The large black hole case shows an initial increase in entanglement entropy, following the Page curve, but displays a discontinuity at the Page time due to a phase transition, as indicated in Fig. 10(a). The intermediate black hole scenario exhibits minimal phase transition effects, with unstable black holes transitioning to smaller phases before the Page time, as marked in Fig. 10(b). The SBH scenario experiences no phase transition, and its Page curve follows the typical pattern of an evaporating black hole, as shown in Fig. 10(c). This anomaly phenomenon leads us to consider the preservation of the information charge Q in the black hole evaporation process. In the mainstream research of the black hole information paradox, information is not lost. Thus, the charge should undergo some physical process to determine its residue or evaporation.

We find that the discontinuity observed in Fig. 10(a) could indicate a physical event, potentially neutralizing the charge and transforming the black hole into an evaporating Schwarzschild black hole, which ultimately dissipates entirely. This process could also influence the replica trick used to compute entropy, as it may prolong the duration on the Hawking saddle prior to transitioning to the wormholes

saddle. Additionally, one can consider the effect of charge Q in the path integral of the replica trick. Such an information problem presents an intriguing avenue for future research.

We conclude that phase transitions indeed impact the Page curve. These transitions may occur before or after the Page time, depending on the initial size of the black hole. Nonetheless, these results do not compromise the unitarity principle of the quantum system, indicating that the paradox can be resolved under these conditions. A prospective research direction could involve examining the mechanisms by which the charge dissipates to zero in RN-AdS black holes coupled with a bath. One interesting aspect is that entanglement entropy might have a relation with the heat engine. The Hawking saddle and replica wormholes saddle may correspond to the liquid or gas phase transition. The parameter to explain the real phase transition could be Renyi entropy or others.

ACKNOWLEDGMENTS

We would like to thank YuQi Lei, ChengYuan Lu and ChenYang Dong for helpful discussions. This work is partly supported by the National Natural Science Foundation of China (Grant No. 12275166 and No. 12311540141).

-
- [1] S. W. Hawking, Breakdown of predictability in gravitational collapse, *Phys. Rev. D* **14**, 2460 (1976).
 - [2] S. W. Hawking, Particle creation by black holes, *Commun. Math. Phys.* **43**, 199 (1975); *Commun. Math. Phys.* **46**, 206 (E) (1976).
 - [3] A. Almheiri, T. Hartman, J. Maldacena, E. Shaghoulian, and A. Tajdini, The entropy of Hawking radiation, *Rev. Mod. Phys.* **93**, 035002 (2021).
 - [4] Giddings, B. Steven, Turiaci, and J. Gustavo, Wormhole calculus, replicas, and entropies, *J. High Energy Phys.* **09** (2020) 194.
 - [5] A. Almheiri, T. Hartman, J. Maldacena, E. Shaghoulian, and A. Tajdini, Replica wormholes and the entropy of Hawking radiation, *J. High Energy Phys.* **05** (2020) 013.
 - [6] G. Penington, S. H. Shenker, D. Stanford, and Z. B. Yang, Replica wormholes and the black hole interior, *J. High Energy Phys.* **03** (2022) 205.
 - [7] D. N. Page, Information in black hole radiation, *Phys. Rev. Lett.* **71**, 3743 (1993).
 - [8] G. Penington, Entanglement wedge reconstruction and the information paradox, *J. High Energy Phys.* **09** (2020) 002.
 - [9] A. Almheiri, N. Engelhardt, D. Marolf, and H. Maxfield, The entropy of bulk quantum fields and the entanglement wedge of an evaporating black hole, *J. High Energy Phys.* **12** (2019) 063.
 - [10] A. Almheiri, R. Mahajan, J. Maldacena, and Y. Zhao, The Page curve of Hawking radiation from semiclassical geometry, *J. High Energy Phys.* **03** (2020) 149.
 - [11] A. Almheiri, R. Mahajan, and J. Maldacena, Islands outside the horizon, *arXiv:1910.11077*.
 - [12] D. Marolf and H. Maxfield, Transcending the ensemble: Baby universes, spacetime wormholes, and the order and disorder of black hole information, *J. High Energy Phys.* **08** (2020) 044.
 - [13] S. W. Hawking, Black hole explosions?, *Nature (London)* **248**, 30 (1974).
 - [14] D. Page, Average entropy of a subsystem, *Phys. Rev. Lett.* **71**, 1291 (1993).
 - [15] X. H. Ge and Y. G. Shen, Reconsidering the black hole final state in Dirac fields, *Phys. Lett. B* **612**, 61 (2005).
 - [16] S. Colin-Ellerin, X. Dong, D. Marolf, M. Rangamani, and Z. Wang, Real-time gravitational replicas: Formalism and a variational principle, *J. High Energy Phys.* **05** (2021) 117.
 - [17] D. Marolf and H. Maxfield, Observations of Hawking radiation: The Page curve and baby universes, *J. High Energy Phys.* **04** (2021) 272.
 - [18] S. Ryu and T. Takayanagi, Holographic derivation of entanglement entropy from AdS/CFT, *Phys. Rev. Lett.* **96**, 181602 (2006).

- [19] V.E. Hubeny, M. Rangamani, and T. Takayanagi, A covariant holographic entanglement entropy proposal, *J. High Energy Phys.* **07** (2007) 062.
- [20] T. Faulkner, A. Lewkowycz, and J. Maldacena, Quantum corrections to holographic entanglement entropy, *J. High Energy Phys.* **11** (2013) 074.
- [21] N. Engelhardt and A. Wall, Quantum extremal surfaces: Holographic entanglement entropy beyond the classical regime, *J. High Energy Phys.* **01** (2015) 073.
- [22] X.H. Ge and Y.G. Shen, Entropy in the NUT-Kerr-Newman black holes due to an arbitrary spin field, *Classical Quantum Gravity* **20**, 3593 (2003).
- [23] K. Hashimoto, N. Iizuka, and Y. Matsuo, Islands in Schwarzschild black holes, *J. High Energy Phys.* **06** (2020) 085.
- [24] X. Wang, R. Li, and J. Wang, Islands and Page curves of Reissner-Nordström black holes, *J. High Energy Phys.* **04** (2021) 103.
- [25] C.Z. Guo, W.C. Gan, and F.W. Shu, Page curves and entanglement islands for the step-function Vaidya model of evaporating black holes, *J. High Energy Phys.* **05** (2023) 042.
- [26] M.H. Yu, X.H. Ge, and C.Y. Lu, Page curves for accelerating black holes, *Eur. Phys. J. C* **83**, 1104 (2023).
- [27] M.H. Yu, C.Y. Lu, X.H. Ge, and S.J. Sin, Island, Page curve, and superradiance of rotating BTZ black holes, *Phys. Rev. D* **105**, 066009 (2022).
- [28] M.H. Yu and X.H. Ge, Islands and Page curves in charged dilaton black holes, *Eur. Phys. J. C* **82**, 14 (2022).
- [29] M.H. Yu and X.H. Ge, Entanglement islands in generalized two-dimensional dilaton black holes, *Phys. Rev. D* **107**, 066020 (2023).
- [30] M.H. Yu and X.H. Ge, Geometric constraints on Page curves: Insights from island rule and quantum focusing conjecture, [arXiv:2405.03220](https://arxiv.org/abs/2405.03220).
- [31] B. Ahn, S.E. Bak, H.S. Jeong, K.Y. Kim, and Y.W. Sun, Islands in charged linear dilaton black holes, *Phys. Rev. D* **105**, 046012 (2022).
- [32] H.S. Jeong, K.Y. Kim, and Y.W. Sun, Entanglement entropy analysis of dyonic black holes using doubly holographic theory, *Phys. Rev. D* **108**, 126016 (2023).
- [33] H. Geng, Replica wormholes and entanglement islands in the Karch-Randall braneworld, [arXiv:2405.14872](https://arxiv.org/abs/2405.14872).
- [34] L. Cheng, X.H. Ge, and S.J. Sin, Anisotropic plasma at finite $U(1)$ chemical potential, *J. High Energy Phys.* **07** (2014) 083.
- [35] A. Ghosh and C. Bhamidipati, Contact geometry and thermodynamics of black holes in AdS spacetimes, *Phys. Rev. D* **100**, 126020 (2019).
- [36] C.Y. Lu, M.H. Yu, X.H. Ge, and L.J. Tian, Page curve and phase transition in deformed Jackiw-Teitelboim gravity, *Eur. Phys. J. C* **83**, 215 (2023).
- [37] R. Jackiw, Lower dimensional gravity, *Nucl. Phys.* **B252**, 343 (1985).
- [38] C. Teitelboim, Gravitation and Hamiltonian structure in two space-time dimensions, *Phys. Lett.* **126B**, 41 (1983).
- [39] S. Cao, Y.C. Rui, and X.H. Ge, Thermodynamic phase structure of complex Sachdev-Ye-Kitaev model and charged black hole in deformed JT gravity, [arXiv:2103.16270](https://arxiv.org/abs/2103.16270).
- [40] A. Chamblin, R. Emparan, C.V. Johnson, and R.C. Myers, Charged AdS black holes and catastrophic holography, *Phys. Rev. D* **60**, 064018 (1999).
- [41] C. Holzhey, F. Larsen, and F. Wilczek, Geometric and renormalized entropy in conformal field theory, *Nucl. Phys.* **B424**, 443 (1994).
- [42] E. Bianchi and M. Smerlak, Entanglement entropy and negative energy in two dimensions, *Phys. Rev. D* **90**, 041904 (2014).
- [43] P. Hayden and J. Preskill, Black holes as mirrors: Quantum information in random subsystems, *J. High Energy Phys.* **09** (2007) 120.
- [44] S.W. Hawking and D.N. Page, Thermodynamics of black holes in anti-de Sitter space, *Commun. Math. Phys.* **87**, 577 (1983).
- [45] H. Eom, S. Jung, and W. Kim, Hawking-Page phase transition of the Schwarzschild AdS black hole with the effective Tolman temperature, *J. Cosmol. Astropart. Phys.* **09** (2022) 053.
- [46] D. Kubiznak and R.B. Mann, P-V criticality of charged AdS black holes, *J. High Energy Phys.* **07** (2012) 033.
- [47] J.V. Rocha, Evaporation of large black holes in AdS: Coupling to the evaporon, *J. High Energy Phys.* **08** (2008) 075.
- [48] H. Geng, Open AdS/CFT via a double trace deformation, [arXiv:2311.13633](https://arxiv.org/abs/2311.13633).
- [49] H. Geng, Graviton mass and entanglement islands in low spacetime dimensions, [arXiv:2312.13336](https://arxiv.org/abs/2312.13336).
- [50] D.N. Page, Hawking radiation and black hole thermodynamics, *New J. Phys.* **7**, 203 (2005).
- [51] R.A. Konoplya, A.F. Zinhailo, and Z. Stuchlík, Quasi-normal modes, scattering, and Hawking radiation in the vicinity of an Einstein-dilaton-Gauss-Bonnet black hole, *Phys. Rev. D* **99**, 124042 (2019).